XPS Studies of Chemically Modified Banana Fibers

L. A. Pothan,*,† F. Simon,‡ S. Spange,§ and S. Thomas⊥

Post Graduate Department of Chemistry, Bishop Moore College, Mavelikkara, Kerala, India, Leibniz Institute of Polymer Research, Hohe Strasse 6, D-01069 Dresden, Germany, Department of Polymer Chemistry, Chemnitz University, Strasse der Nationen 62, D-09107 Chemnitz, Germany, and School of Chemical Sciences, Mahatma Gandhi University, Priyadarsini Hills P.O, Kottayam, Kerala, India

Received July 1, 2005; Revised Manuscript Received December 6, 2005

Banana fibers obtained from the sheath of the banana plant (*Musa Sapientum*) whose major constituent is cellulose were modified using various chemical agents in order to improve their compatibility with the polymer matrix. The change in the surface composition of the raw and chemically modified fiber was investigated using various techniques such as solvatochromism, electrokinetic measurements, and XPS. Surface characterization by XPS showed the presence of numerous elements on the surface of the fiber. Investigation of the surface after alkali treatment on the other hand showed the removal of most of the elements. Silane treatment was found to introduce a considerable amount of silicon on the surface of the fiber. The [O]/[C] ratio was found to decrease in all cases except for the fluorinated and vinyl silane treated fibers. Detailed investigation of the deconvoluted C 1s spectra revealed the change in the percentage atomic concentration of the various elements on the fiber surface. The dissolution of the various surface components by alkali treatment, which was earlier revealed by SEM, was further confirmed by XPS. The XPS results were found to perfectly agree with the solvatochromic and electrokinetic measurements.

Introduction

X-ray photoelectron spectroscopy (XPS), which involves the measurement of the binding energies of electrons ejected by the ionizations of atoms with a monoenergetic beam of soft X-rays, has widely been used for the surface characterization of wood, wood pulp cellulose, and polymers.[1−3] The XPS technique, developed by Siegbahn and co-workers,[4,5] provides a unique tool for the investigation of a solid surface. Although X-rays penetrate deep into a sample, the XPS technique is very sensitive to surface constituents. Electrons emitted from the bulk of the material lose their energy with a high probability through collisions with electron orbitals of the bulk atoms. As a result, only atoms in a surface layer of very limited depth contribute to the intensity of the measured electron emission. Hence, the information depth of the method depends on the element which is under investigation, the quantum energy of the X-ray source ($h\nu$), and the angle of incidence.[6] In the case of the widely employed weak Al Kα X-rays the information depth is ca. 10 nm which is the maximum for the C 1s level.

The kinetic energy (E_{kin}) of the emitted electrons (so-called photoelectrons) or their corresponding binding energy ($E_{bin} = h\nu - E_{kin}$) characterizes the elements present in the surface layer, and the intensity of the signal indicates their quantity. Furthermore, the energy of electrons emitted from a given element shell may be altered, depending on the type of chemical bond formed by the element. Therefore, on the basis of the possible chemical shift of the binding energy of a given element, the type of chemical bond present in the surface can be determined.

Gellerstedt and Gatenholm[7] characterized succinylated lignocellulosic fibers using XPS. The results showed that carboxylic functionalities are predominantly introduced at the fiber surface. The surface properties of the modified chemical pulp, as measured by XPS, showed that the fiber surfaces are modified to a higher extent than the cell wall. Liu et al.[8] used XPS to study the effect of alkali treatment on the structure of native grass fibers. The inside and outside surfaces of the fibers were examined separately. Survey scans for each material revealed carbon, oxygen, nitrogen, and calcium. Cai et al.[9] studied the effect of surface-grafted ionic groups on the performance of cellulose fiber reinforced thermoplastic composites. The elements present on the fiber surface were detected using XPS analysis. It has been found that atomic ratio of O/C slightly increased on fiber treatment. A solid-state NMR and XPS study of ethylene vinyl acetate−ethylene vinyl alcohol copolymer (EVA)/sugarcane composites was carried out by Tavares et al.[10] The results of the quantitative surface analysis of the composites revealed the presence of elements C, O, Si, and N. Hassan et al.[11] studied the effect of silane monomer on the improvement of the mechanical and degradable properties of photografted jute yarn with acryl amide. The surfaces of the treated and untreated fibers were characterized using XPS. It has been ascertained by the XPS studies that a chemical reaction has taken place with the cellulose backbone of the jute fiber. The effect of acetylation and propionylation surface treatments on natural fibers was investigated by Tserki et al.[12] The O/C ratio of the various treated and untreated fibers was studied. The surface of the untreated fiber was found to have an O/C ratio close to that of waxes showing that the fiber surface is covered with waxes. The surface characterization of argon and air plasma treated wood fibers carried out by Yuan et al.[13] by XPS studies showed that air plasma treatment improves the O/C ratio more than that of the argon plasma treated wood.

Banana fibers obtained from the pseudo stem of the banana plant have high cellulose content and have been found to be effective reinforcement in polymeric matrixes.[14] However, one defect associated with the fibers is their high hydrophilicity as

* To whom correspondence should be addressed. E-mail: lalyaley@yahoo.co.uk.
† Bishop Moore College.
‡ Leibniz Institute of Polymer Research.
§ Chemnitz University.
⊥ Mahatma Gandhi University.

10.1021/bm050462a CCC: $33.50
Published on Web 02/14/2006

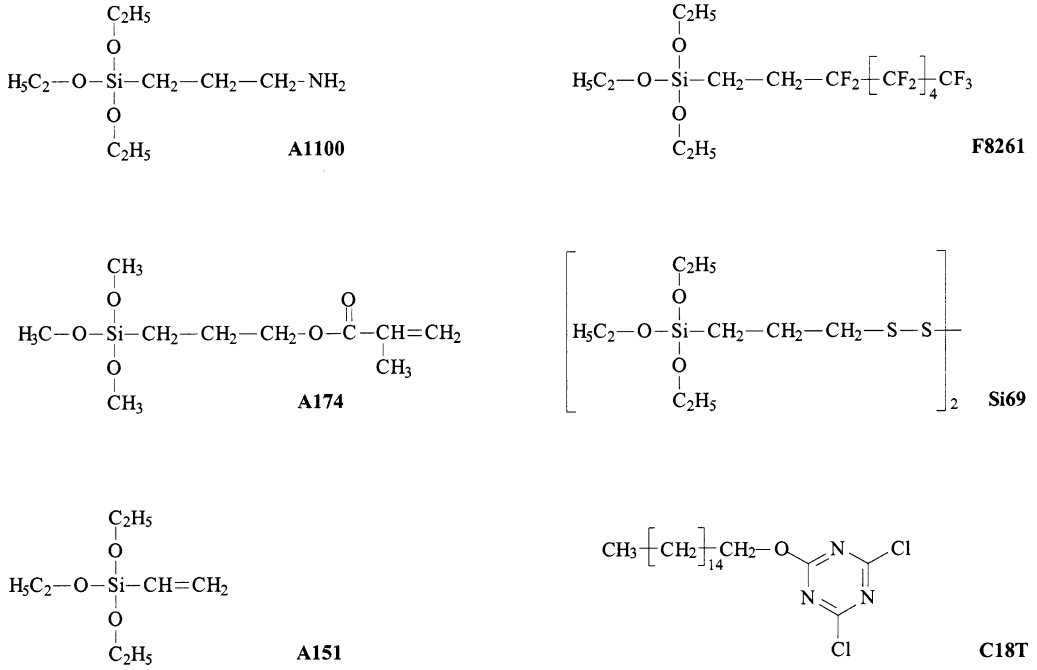

Figure 1. Substances employed to modify the banana fiber surfaces: A1100 = (3-aminopropyl)triethoxysilane, A174 = γ-methacryl oxypropyltrimethoxysilane, A151 = vinyl triethoxysilane, F8261 = 1H,1H,2H,2H-perfluorooctyl triethoxysilane (Dynasylan), Si69 = bis(3-triethoxysilylpropyl)-tetrasulfone, and C18T = 2,4-dichloro-6-*n*-octadecyloxy-1,3,5-triazine.

well as the weak interfacial bond with polymeric matrices. Chemical modification has been found to be effective in improving the compatibility of the fiber with the matrix. Silane treatment, found to be effective in the case of glass fibers, was used in this case also since the hydroxyl groups of the cellulose fibers are prone to chemical reactions when proper reagents are used. Sodium hydroxide, found to be effective with other natural fibers for surface modification, was used in the present case. In this communication, XPS has been used as a tool to evaluate the surface of the banana fibers. The results were found to be perfectly consistent with our earlier observations by other techniques.

Experimental Section

Materials Used. Banana fibers were obtained from Sheeba Fibers and Handicrafts, Poovancode, Tamil Nadu, India. The various silanes, (3-aminopropyl)triethoxysilane (A1100), γ-methacryloxypropyltrimethoxysilane (A174), and vinyl triethoxysilane (A151), were obtained from Sigma-Aldrich, India. 1H,1H,2H,2H-Perfluorooctyl triethoxysilane (Dynasylan, F8261) was obtained from ABCR GmbH. Bis(3-triethoxysilylpropyl)-tetrasulfide (Si69) was obtained from Degussa AG, Germany. 2,4-Dichloro-6-*n*-octadecyloxy-1,3,5-triazine (C18T) was synthesized in the laboratory according to Zadorecki and Flodin.[15] The chemical structures of the various chemical agents used are shown in Figure 1. NaOH, acetic anhydride, and all other chemicals were of commercial grade.

Treatment with NaOH. The raw banana fibers obtained from local sources by mechanical separation of the fiber from the stem were cleaned and refluxed in a 0.25% solution of NaOH for 1 h and then washed in very dilute acid to remove the nonreacted alkali. Washing was continued until the fibers were alkali free. The washed fibers were then dried in an oven at 70 °C for 3 h.

Treatment with Acetic Anhydride. The fibers were dipped in glacial acetic acid for 30 min. The acid was drained, and the fibers were dipped in acetic anhydride containing a few drops of concentrated sulfuric acid for 5 min. Then, the fibers were washed in distilled water and dried.

Silane Treatment for Banana Fibers. A 0.6% solution of the silane in ethanol/water mixture in the ratio of 6:4 was prepared, and the solution was allowed to stand for an hour. The pH of the solution was maintained at 4 by adding acetic acid. Neatly separated and cut banana fibers were dipped in the above solution and were allowed to remain there for $1^1/_2$ hours. The ethanol/water mixture was drained out, and the fibers were dried in air for half an hour followed by drying in an oven at 70 °C until the fiber was fully dry.

Treatment with Triazine Coupling Agent (C18-T). The triazine coupling agent 2,4-dichloro-6-*n*-octadecyloxy-1,3,5-triazine (C18T) was synthesized according to the procedure described by Zadorecki and Rouhult.[16] The dried cellulose fibers were first immersed in 0.1 mol·L^{-1} NaOH solution, dried, and then soaked in a solution of C18-T (10 wt % of the fibers) in acetone for 3 min at room temperature. After evaporation of the solvent the fibers were dried at 60 °C for 2 h in an inert atmosphere.

Fiber Surface Characterization. *X-ray Photoelectron Spectroscopy (XPS).* All XPS studies were carried out by means of an AXIS ULTRA photoelectron spectrometer (KRATOS ANALYTICAL, Manchester, United Kingdom). The spectrometer was equipped with a monochromatic Al Kα X-ray source ($h\nu$ = 1486.6 eV) of 300 W operating at 15 kV. The kinetic energy of the photoelectrons was determined with a hemispherical analyzer set to pass energy of 160 eV for the survey spectra and of 20 eV for high-resolution spectra, respectively. During all measurements, electrostatic charging of the sample was overcompensated by means of a low-energy electron source working in combination with a magnetic immersion lens. Later, all recorded peaks were corrected for electrostatic charging by setting the component peak of the saturated hydrocarbons in the C1s spectrum to 285.00 eV. In all experiments the base pressure in the analysis chamber was less than 10^{-8} mbar.

Quantitative elemental compositions were determined from peak areas using experimentally determined sensitivity factors and the spectrometer transmission function. Spectrum background was subtracted according to Shirley.[17] The high-resolution spectra were dissected by means of a special deconvolution software package. The free parameters of component peaks were their binding energy (BE), height, full width at half-maximum (fwhm), and the Gaussian/Lorentzian ratio.

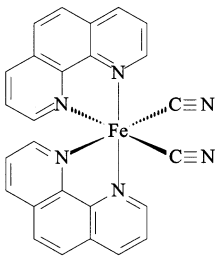

1

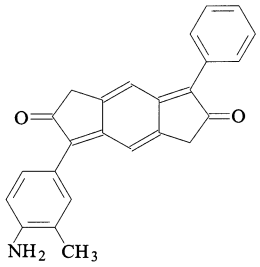

2

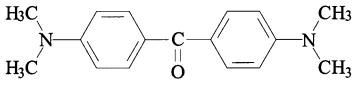

3

Figure 2. Solvatochromic dyes employed to characterize banana fibers' Lewis acidity/basicity and polarity: **1** = *cis*-dicyano-bis(1,10-phenanthroline)-ferric [$Fe(phen)_2(CN)_2$], **2** = 3-(4-amino-3-methylphenyl)-7-phenyl-2,6-dihydrofurano[2′,3′:4,5]benzofuran-2,6-dion (ABF), **3** = 4,4′-bis(*N*,*N*-dimethylamino)benzophenone (Michler's ketone).

Electrokinetic Measurements. Electrokinetic measurements were carried out to determine the zeta-potential (ζ) of fiber surfaces. The electrokinetic analyzer EKA (Anton Paar KG, Graz, Austria) was based on the streaming potential method. An electrolyte solution was forced by an external pressure p through a bundle of capillaries (fiber plug). The potential U resulting from the motion of ions in the diffuse layer was measured with respect to the applied pressure. The electrokinetic potential or zeta-potential (ζ) was calculated from the measured streaming potential using Smoluchwski's equation ($\Delta U/\Delta p$). During swelling, the ions present in the fiber are incorporated into the swollen layer and influence the surface conductivity. Hence, the calculated zeta-potential must be considered as an apparent zeta-potential (ζ_{app}).The details of the measuring technique are reported elsewhere.[18] By measuring the pH dependence of the zeta-potential, the Brønsted acidity or basicity of solid surfaces can be determined qualitatively.

Solvatochromic Measurements. Certain dyes can be used as probe molecules to characterize the Lewis acid−base properties as well as the polarity of solid surfaces.[19−22] In an extensive experimental study, Spange et al. showed that *cis*-dicyano-bis(1,10-phenanthroline)-iron [$Fe(phen)_2(CN)_2$] (**1**) can be used as an indicator to quantify a solid's surface acidity α.[19] The indicator 3-(4-amino-3-methylphenyl)-7-phenyl-2,6 dihydrofurano [2′,3′:4,5] benzofuran-2,6-dion (ABF) (**2**) is sensitive for surface basicity β, and Michler's ketone (4,4′-bis(*N*,*N*-dimethylamino)benzophenone) (**3**) allows one to estimate a surface's dipolarity/polarizability π^* (Figure 2).[20] However, the interaction of a solid surface with a solvatochromic dye is the result of many effects. Acid−base, dipole−dipole, induced dipole−dipole, dispersion, and structural forces contribute to the overall adsorption free energy of a probe dye with the solid surface. This means that for each UV−vis spectrum taken from an adsorbed solvatochromic dye, surface sites of different polarity as well as different contributions of specific (acid−base) and nonspecific (dipolar−polarizable) interactions must be taken into account. Figure 3 shows typical acid/base interaction sites on a cellulose surface.

The fibers were weighed and covered with 20 mL of the respective solvent. Stock solutions of the probe dyes of the specified concentration were prepared. In the case of dye **1** a concentration of 2×10^{-3} mol·L^{-1} in 1,2-dichloroethane (DCE) was used, and for dyes **2** and **3** a concentration 1×10^{-3} mol·L^{-1} in cyclohexane was used. The required amount of the stock solution (4 mL for **1**, 2 mL for **2** and **3**) was added to the fibers in the respective solvent (DCE or cyclohexane). The fibers with the probe dyes were kept vibrating overnight. Then the solvent was decanted off, and the fibers were washed with the respective solvents to remove any adhering dye particles. The fibers were dried in a vacuum at 30 °C for 12 h. The dried samples were used for UV−vis measurements. The equipment employed was a UV−vis spectrometer MCS 400 with glass fiber optics (ZEISS GmbH). UV−vis spectra of fibers were recorded by a special reflectance technique (more details are given in ref 19). The fibers were placed between two quartz plates. The sensor head for measuring reflectance spectra was located under one of these quartz plates, and the UV−vis spectrum of the adsorbed dye was monitored. The absorption maxima were detected with a software program.

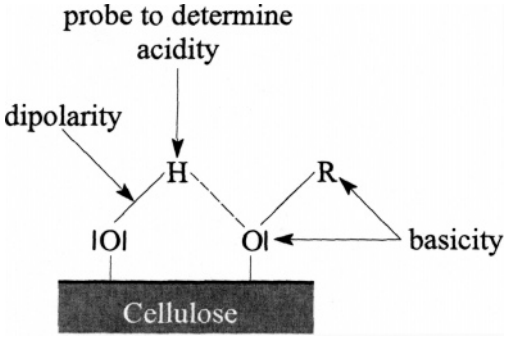

Figure 3. Typical acid/base interaction sites on a cellulose surface and their possible interactions with the different solvatochromic dyes.

To determine the Kamlet−Taft parameters α, β, and π^*, the measured solvatochromic shift of dye's absorption band ν_{max}(probe) was substituted in the empirical linear solvatation energy relationship (eq 1):[19]

$$\nu_{max}(\text{probe}) = \nu_{max}(\text{solv}) + a\alpha + b\beta + s(\pi^* + d\delta) \quad (1)$$

The ν_{max}(solv) parameter is the solute property of a reference system (here, the dye dissolved in DCE or cyclohexane), δ is a polarizability correction term which is 1.0 for aromatic, 0.5 for polyhalogenated, and 0 for aliphatic solvents. The values a, b, s, and d are solvent-independent correlation coefficients.

Results and Discussions

XPS Studies. *Elemental Surface Composition.* The chemical composition of surfaces of raw and chemically modified fibers was investigated using XPS. Banana fibers, obtained from the pseudo stem of the banana plant, are of natural origin. The fibers, in addition to providing strength for the supporting structures, also serve as carriers of water and nutrients. The plant fibers as such are a composite of cellulose, hemicellulose, lignin, and waxes. Hence, it is not surprising that many elements were detected on the raw banana fiber surface. Besides the elements forming the so-called living matter as carbon, nitrogen, and oxygen, the fibers contain inorganic elements, such as magnesium, aluminum, potassium, calcium, and silicon. Furthermore, phosphorus and chlorine were detected (Figure 4a). Traces of fluorine which have been noticed can be believed to have been incorporated during fiber processing and cutting and also as nutrients.

Table 1 shows the elemental composition in the untreated and variously treated fibers obtained from the survey spectra.

It has been found that the aluminosilicates as well as Mg have been dissolved by NaOH. In the case of aluminosilicates containing magnesium, NaOH would destroy the silicate lattice and remove the formed aluminum and silicon ions, but usually the magnesium will remain on the sample surface. The loss in the [N]/[C] ratio shows that the organic matrix of the fiber surface is affected in the strong basic environment. The small decrease in the [O]/[C] ratio can be attributed to the dissolution of hemicellulose and lignin after alkali treatment. The dissolution

Table 1. Elemental Composition of Untreated and Variously Treated Fibers Obtained from the Survey Spectra

sample	[N]/[C]	[O]/[C]	[F]/[C]	[Mg]/[C]	[Al]/[C]	[Si]/[C]	[P]/[C]	[S]/[C]	[Cl]/[C]	[K]/[C]	[Ca]/[C]
untreated	0.033	0.654	0.020	0.009	0.013	0.007	0.002		0.001	0.013	0.007
NaOH-treated	0.015	0.590									
acetylated	0.029	0.628	0.115			0.009					
A1100	0.014	0.266	0.023			0.099					0.010
A174	traces	0.476				0.096					
A151	0.006	0.757				0.259					
F8261	0.028	0.673	0.226		0.009	0.031					0.004
Si69	0.019	0.514				0.125		0.191			
C18T	0.060	0.125				0.026			0.013		

of the lignin component with a high [O]/[C] ratio results in an overall lowering of the same.

The acetylation of the C−OH groups of the cellulose not only prevents the formation of inter- and intramolecular hydrogen bridge linkages, it is also a way to lower the polarity and enhance the compatibility to polyolefin matrixes. Table 1 shows that the ester formation does not significantly change the surface composition.

The banana fibers were treated with silanes to introduce various functional groups on the fiber surface. According to the mechanism as shown in Figure 5 the silicon is introduced on the surface revealing that the reaction with the silane on the surface has occurred.

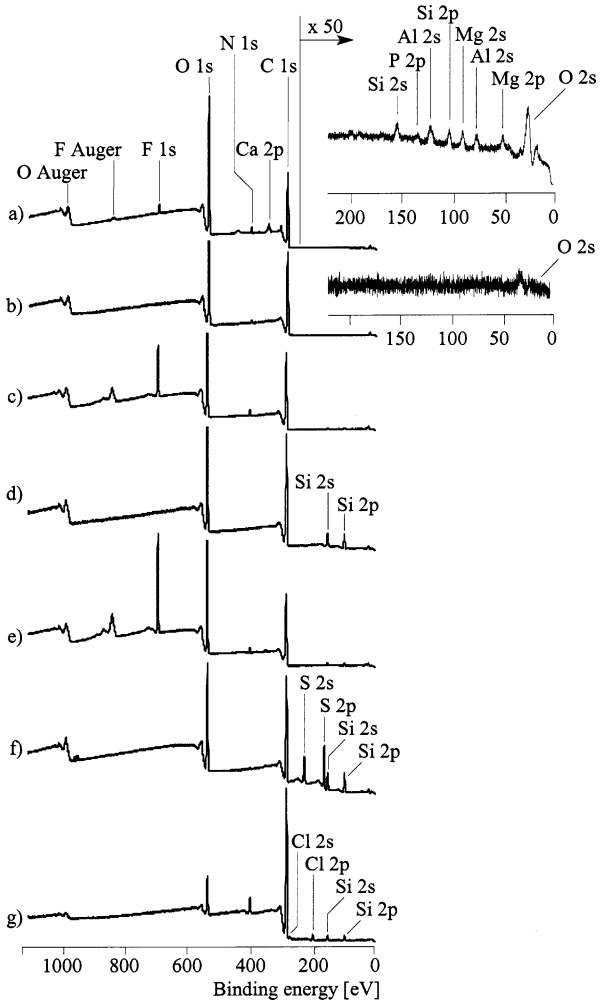

Figure 4. Series of XPS survey spectra of raw and chemically modified banana fibers: untreated banana fibers (a), fibers after a treatment with 0.25% NaOH (b), fibers after acetylation (c), fibers grafted with the silane A174 (d), fibers grafted with the fluorosilane F8261 (e), fibers grafted with the sulfur-containing silane Si69 (f), and fibers treated with C18T (g). The insets are cuts of the survey spectra of untreated (a) and NaOH-treated (b) banana fibers showing the presence or absence of accompanying elements in the sample surfaces.

While the reactions with the silanes F8261, A174, and A151 worked excellently ([Si]/[C] ratios in Table 1), the degree of reaction of A1100 was rather low. In comparison to the untreated fiber a lower [N]/[C] ratio was found. But the [N]/[C] ratios determined from the survey spectra are not sensitive to determine the number of introduced amino groups because the N 1s signal in the survey spectra collects all nitrogen-containing species, like amines, amides, peptides, etc. The discussion of the deconvoluted C 1s spectrum below shows that the A1100-treated fiber surface contains a considerable number of amino groups. The grafting of the semifluorinated silane F8261 introduces a high amount of fluorine on the fiber surface. In this way it seems possible to produce fiber surfaces with a strong hydrophobic character. The sulfur-containing silane Si69 introduced a considerable amount of sulfur in the fiber surface. The sulfide can act as adhesion promoter for rubber and other polymers containing double bonds which can be opened by an oxidation in the presence of sulfur. Investigation of the C18T-treated fibers showed the presence of high hydrocarbon content, which appears mainly from the long stearyl chain bonded via an ether bridge on the triazine. The nitrogen content is low because the alkyl chains cover the triazine headgroup, which is obviously direct in the contact to the fiber surface (Figure 6).

High-Resolution C 1s Spectra. High-resolution XPS spectra can be used for the chemical characterization of surfaces. The spectrum deconvolution allows identification of functional surface groups which can be as an anchor for further derivatization reaction or the formation of covalent bonds to a wrapping polymer matrix. In addition, good compatibility between fiber and polymer matrix requires the knowledge of the kind and number of the interacting species.

The C 1s spectra shown in Figure 7 have a rather complex structure resulting from the natural origin of the samples.

The C 1s spectrum of the untreated fiber clearly shows the shape of a polysaccharide (cellulose material). The spectrum is deconvoluted into seven component peaks indicated by letters in italic style (*A*, *B*, *C*, etc.). The polysaccharides are presented by the component peaks *C* and *D* appearing from the *C*−OH and acetal (O−*C*−O) groups, respectively. The ratio of the two component peak areas [*D*]/[*C*] = 1:5 corresponds to the stoichiometric [*C*−OH]/[O−*C*−O] ratio of cellulose. Component peak *A* shows the presence of considerable amounts of hydrocarbons (C_xH_y). Component peak *B* presents all amines (*C*−N) but does not contain carbon atoms in the β-position (*C*−COOH) of carboxylic acid groups that are shown by component peak *F*. The area of component peak *B* equals the [N]/[C] ratio determined from the survey spectrum. Hence, it can be assumed that only primary amines, amides, or peptides contribute to *B*. In the case of polysaccharide structures the

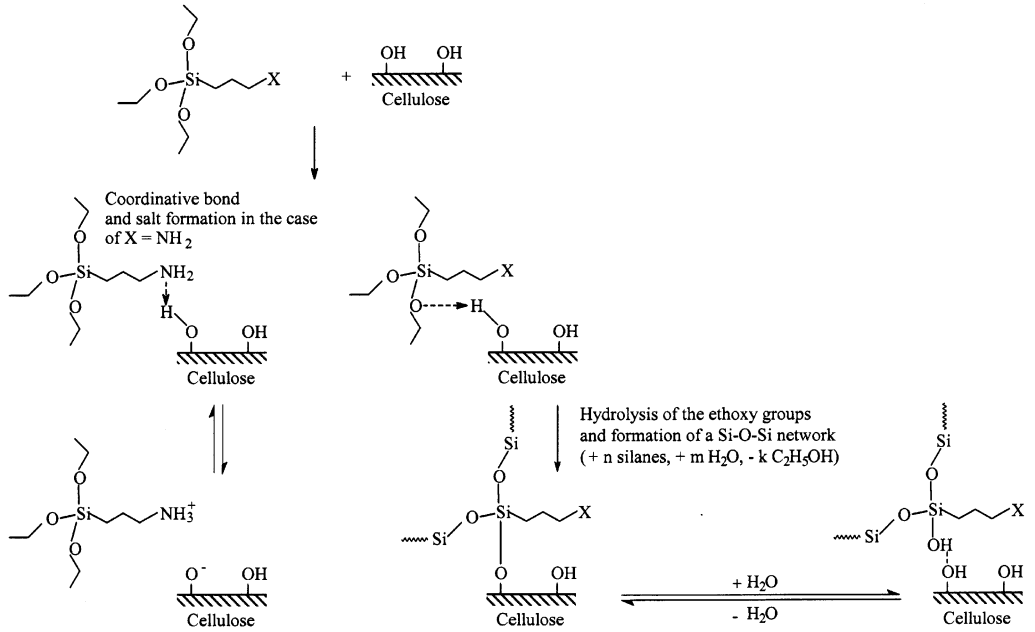

Figure 5. Scheme of interaction of silanes with cellulose. In addition to the self-condensation of silanes and the condensation on the cellulose fiber surface, amino silane molecules can interact with the cellulose's OH groups via their Brønsted basic amino groups.

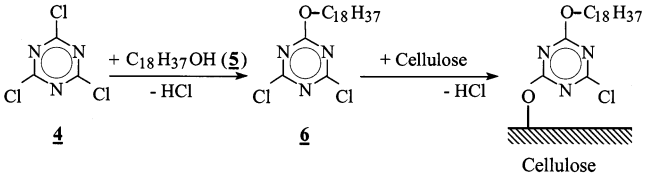

Figure 6. Scheme of preparation of C18T and its interaction with cellulose (**4**, 2,4,6-trichloro-1,3,5-triazine; **5**, steryl alcohol; **6**, 2,4-dichloro-6-*n*-octadeyloxy-1,3,5-triazine, C18T).

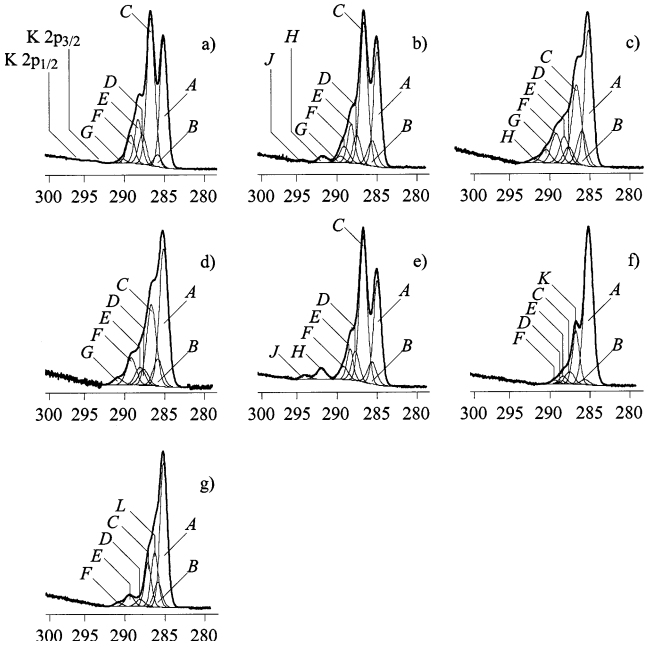

Figure 7. Deconvoluted C1s spectra of the variously treated fibers: untreated banana fibers (a), fibers after acetylation (b), fibers grafted with the silane A1100 (c), fibers grafted with the silane A174 (d), fibers grafted with the fluorosilane F8261 (e), fibers grafted with the sulfur-containing silane Si69 (f), and fibers treated with C18T (g). The component peaks indicated by letters in italic style are explained in the text.

carbons situated in the β-position to the electronegative carbonic acid or ester groups have an oxygen atom in its immediate neighborhood and contribute to component peaks at higher binding energies. The binding energy of component peak *E* is in the lower range of esters, but its nature can be better explained by keto groups (>*C*═O) and amide or peptide bonds (HN−*C*═O). In the case of esters (O═*C*−O−C) a corresponding ether carbon O═C−O−*C*) has to be observed that contributes to the component peak *C*. However, the area of *C* agrees excellently with the stoichiometry of the cellulose. Component peak *G* appears from carbon atoms bonded to fluorine (*C*−F) or from inorganic carbonates (CO_3^{2-}) which have been introduced by Ca, K, Mg, etc.

The C 1s spectrum of the sample subjected to acetylation is similar to the C 1s spectrum (Figure 7b) of the untreated fiber. Its component peaks are explained above. Two new component peaks *H* and *I* are observed. Both appear from C−F bonds, where component peak *H* appears from CF_2 groups and *I* from CF_3. Surprisingly, the intensities of the two peaks are found to be low and do not correspond with the atomic [F]/[C] ratio determined from the survey spectrum. Probably the fluorinated component is decomposed under X-ray irradiation which is typical for many fluorinated and semifluorinated polymers.

The C 1s spectrum of the sample treated with silane A1100 (Figure 7c) shows the same shape discussed above. Hence, the nature of the component peaks agrees with the explanation above. If it is assumed that the component peak *H* appears from CF_2 groups, here, the area of *H* agrees excellently with the [F]/[C] ratio determined from the survey spectrum. Component peak *B* is composed of the carbon atoms in the β-position of the carboxylic acid groups (component peak *F*) and the considerable amount (1.42%) of primary amines.

The treatment of banana fibers with the silane A174 introduces methacrylic esters in the sample surface. Here, the intensive component peak *B* cannot appear only from the small amount of *C*−N bonds (the survey spectrum shows only traces of nitrogen). Obviously, carbon atoms in the β-position of the ester groups (H_2C═*C*H−C (O)−O−C) mainly contribute to this component peak. Hence, the intensity of *B* equals the intensity of *F* showing the presence of ester carbons (H_2C═CH−*C*(O)−

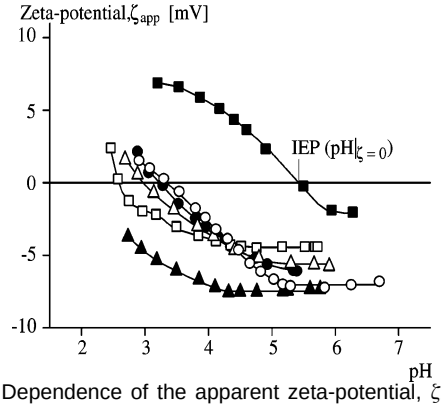

Figure 8. Dependence of the apparent zeta-potential, ζ_{app} on pH values of variously silanized banana fibers: untreated banana fibers (□), fibers grafted with the silane A1100 (■), fibers grafted with the silane A151 (○), fibers grafted with the silane A174 (●), fibers grafted with the fluorosilane F8261 (▲), and fibers grafted with the sulfur-containing silane Si69 (△). All measurements were performed as streaming potential measurements in 10^{-3} mol·L^{-1} KCl.

O−C) (Figure 7d). All other component peaks can be assigned to structures explained for the untreated sample.

The C 1s spectrum (Figure 7e) of the sample treated with the fluorinated silane shows two pronounced component peaks *H* and *J* showing the presence of CF_2 and CF_3 groups. Here, the amount of fluorine, which is calculated from the C 1s spectrum, is also found too low ($[F]/[C]|_{C1s} = 0.113$). It is only half of the fluorine content found in the survey spectrum. Obviously, the fluorinated sequences of the alkyl chains are decomposed during the recording of spectra.

The sample treated with Si69 contains enormous amounts of sulfur. Here, the component peak *K* appears from *C*−S bonds (Figure 7f).

Samples treated with 2,4-dichloro-6-*n*-octadecyloxy-1,3,5-triazine (C18T) show a high amount of saturated hydrocarbons (component peak *A*). The high amount of *C*−N and *C*═N bonds is presented by the component peak *B* that also shows the carbon atoms in the *β*-position of the carboxylic acid groups (component peak *F*). An additional component peak *L* may appear from ether groups (*C*−O−*C*) or alcoholic *C*−OH groups. But usually *C*−OH groups show a stronger chemical shift and were found at BE >286.4 eV[2,23]. An ester component peak (O═*C*−O−C) with an intensity in the range of component peak *L* was not observed. Hence, it cannot be assumed that considerable amounts of esters are on the sample surface.

Electrokinetic Results. Electrokinetic measurements were found to be successful in characterizing the Brønsted acid−base properties of chemically modified banana fibers. Figure 8 shows the pH dependence of the apparent zeta-potential, ζ_{app}. At low pH values the untreated banana fiber is positively charged by its protonated surface groups. The increase of pH lowers the zeta-potential indicating the gradual loss of protonated groups. At a pH = 2.6 the isoelectric point (IEP, pH where the zeta-potential is zero) is found. According to the Stern theory of the electrochemical double layer[24] this point corresponds with the number of Brønsted acid surface sites. Negative zeta-potential values are observed by increase in the pH which promotes the dissociation of these Brønsted acid surface sites. The shape of the ζ_{app} versus pH curve is typical for surfaces with a hydrophilic character. The two plateau phases (first plateau starts at pH ≈ 3.25, second plateau at pH ≈ 4.5) indicate two different surface charging mechanisms, the dissociation of Brønsted acid groups (till the first plateau), here carboxylic groups found in the C 1s spectra (component peak *F* in Figure 7a) followed by the preferable adsorption of OH^- ions on the fiber surface (till the second plateau). The plateaus were reached if all dissociable groups are dissociated or the capacity of OH^- adsorption is used.

All measurements were performed as streaming potential measurements in 10^{-3} mol·L^{-1} KCl. The coupling of the silanes A151 and A174 involves some of the Brønsted acid surface sites and does not introduce new surface functionalities with a pronounced Brønsted acid−base character. Hence, the IEP is slightly shifted to higher pH values. The strongly linear ζ_{app} versus pH dependence indicates a dominant charge formation by an adsorption of OH^- ions on the surface having a lower hydrophilic character. Similar results were obtained in the case of the surface modification by Si69. The sulfide may prevent the moderate hydrophobic character of the other silane-modified fiber surfaces, but it does not act as pronounced Brønsted acid or base.

The silanization with the fluorine-containing silane strongly changes the shape of the ζ_{app} versus pH curve. A protonated surface indicated by positive zeta-potential values was not observed. The introduction of a long semifluorinated alkyl chain should clearly lower the hydrophilic surface character, and only a strong OH^- adsorption should determine the charge formation. The absence of an IEP in the pH region under investigation and the shape of the ζ_{app} versus pH curve indicate a charge formation mechanism by the dissociation of strong Brønsted acid surface groups. During the hydrolyzation of the alkoxysilane molecules, strongly acidic Si−OH groups can be produced. Usually the Si−OH groups are involved in the silica network formation or anchoring on the fiber surface. However, the formation of C−O−Si bonds between the silica network and the fiber surface can be unstable against water. The hydrolyzation of the bonds produces Si−OH groups which can undergo dissociation reactions (Figure 5).Obviously, the fluorinated alkyl chain lowers the stability of the C−O−Si bond, and a relative small amount of silicon was found on the silanized fiber surface (Table 1).

In the case of silane A1100-treated fibers the surface changes to Brønsted basic properties with an IEP of 5.4, obviously due to the effect of the $-NH_2$ groups. The $-NH_2$ groups are able to take up a high number of hydronium ions forming ammonium groups. With increasing pH value, the positively charged ammonium groups were gradually deprotonated and the zeta-potential decreases. An IEP of 5.4 is rather small for amino-silanized fiber surfaces and shows the presence of a considerable amount of Brønsted acid surface centers besides the Brønsted basic amino groups. The atomic ratios [Si]/[C] and [N]/[C] in Table 1 and component peak *B* in Figure 7c show that the number of the Brønsted basic amino groups is rather small. The hydrolyzation reaction of the C−O−Si bonds between the fiber surface and the silanes (Figure 5) prevents a higher functionalization degree. In contrast to fluorosilanes the aminosilanes can be better solvated, and a silane desorption can take place.

Solvatochromic Measurements. Details of the findings when the modified fiber surfaces were characterized by solvatochromism has been reported elsewhere.[21] The surface Lewis acidity α, the Lewis basicity *β*, and the dipolarity/polarizability *π** were determined in a few cases for the chemically modified cellulose fibers. Table 2 summarizes the parameters for the differently modified banana fibers.

The untreated fiber surface shows a moderate Lewis acidity and a rather low polarity. The NaOH treatment removes the silica skeleton and other metal ions. Hence, the Lewis acidity α is slightly decreased. The increased polarity can be explained by the damage of the fiber surface and the uncovering of

Table 2. Polarity Parameters of the Differently Modified Banana Fibers

banana fibers	α	β	π^*
untreated	1.57		0.31
0.25% NaOH	1.43	1.07	0.70
0.5% NaOH	1.51		0.74
0.25% NaOH + A174	1.21		0.95
0.5% NaOH + A174	0.99		1.28
0.25% NaOH + A151	1.79	1.27	0.64
0.5% NaOH + A151	1.73		0.53
F8261	1.31	1.46	0.83
Si69	1.29		0.72

cellulose structure. The silanization of the NaOH pretreated surface with A174 additionally lowers the surface acidity by involving the most acid surface groups in the silanization reaction or the shielding by the methacryloxypropyl chains. The introduced ester groups clearly increases the surface polarity. The low π^* value of the fiber surface modified with A151 shows that the π bonds of the vinyl group and probably also the methacryl group in sample A174 do not substantially contribute to surface polarity. The fluorination of the fiber surface by the F8261 modification should strongly lower the surface acidity, basicity as well as polarity. The values found support the findings of the XPS and electrokinetic measurements that the grafted amount of the semifluorinated silane must be very low. The silane self-condensation in the immediate neighborhood to the fiber surface and the formation of strongly acidic Si−OH groups (Figure 5) compensate the expected lowering of the surface Lewis acidity and dipolarity/polarizability.

Conclusion

Surface characterization of raw and chemically modified banana fibers with XPS revealed the presence of surface functionalities. Dissolution of most of the surface elements as evidenced in the SEM, solvatochromic measurements, and electrokinetic measurements was further confirmed by ESCA analysis. Interaction of the fibers with silanes on the surface was further evidenced. However, the grafting rate of silanes is rather low because the formed Si−O−C bond has a high tendency to hydrolyze in the presence of water. Nevertheless, the self-condensation of the silanes and the network formation in the immediate neighborhood of the fiber surface is an excellent tool to functionalize the fiber surface and might be used to enhance the fiber's compatibility to a polymer matrix. It can be also assumed that the reaction products of the silanes contribute to protect the fibers against an unwanted water uptake in composite materials.

Acknowledgment. Helpful discussions with Mrs. B. Anandakutty, Department of Chemistry, Bishop Moore College is respectfully acknowledged.

References and Notes

(1) Barry, A. O.; Riedl, B.; Adnot, A.; Kaliaguine, S. C. *J. Electron Spectrosc. Relat. Phenom.* **1991**, *57*, 47−59.
(2) Kamdem, D. P.; Riedl, B.; Adnot, A.; Kaliaguine, S. C. *J. Appl. Polym. Sci.* **1991**, *43*, 1901−1912.
(3) Chtourou, H.; Riedl, B.; Kokta, B. V. *J. Colloid Interface Sci.* **1993**, *158*, 96−104.
(4) Siegbahn, K.; Hamrin, K.; Hedman, J.; Johansson, G.; Bergmark, T.; Karlsson, S. E.; Lindgren, I.; Lindbert, B. *ESCA: Atomic, Molecular and Solid State Structure by means of Electron Spectroscopy*; Almquist and Wiksells: Uppsala, Sweden, 1967.
(5) Axelson, G.; Ericson, U.; Fahlman, A.; Hamrin, K.; Hedman, J.; Nordberg, R.; Nordling, C.; Siegbahn, K. *Nature* **1967**, *213*, 70−71.
(6) Dorris, G. M.; Gray, D. G. *Cellul. Chem. Technol.* **1978**, *12*, 9−23.
(7) Gellerstedt, F.; Gatenholm, P. *Cellulose* **1999**, *6*, 103−121.
(8) Liu, W.; Mohanty, A. K.; Drzal, L. T.; Askel, P.; Misra, M. *J. Mater. Sci.* **2004**, *39*, 1051−1054.
(9) Cai, X.; Riedl, B.; Ait-Kadi, A. *J. Polym. Sci, Part B: Polym. Phys.* **2003**, *41*, 2022−2032.
(10) Tavares, M. B.; Stael, G. C.; Gorelova, M. M.; De Menezes, S. M. C. *J. Appl. Polym. Sci.* **2001**, *80*, 2120−2122.
(11) Hassan, M. M.; Islam, M. R.; Sawpan, M. A.; Khan, M. A. *J. Appl. Polym. Sci.* **2003**, *89*, 3530−3538.
(12) Tserki, V.; Zafeiropoulos, N. E.; Simon, F.; Panayiotou, C. *Composites, Part A* **2005**, *36*, 1110−1118.
(13) Yuan, X.; Jayaraman, K.; Bhattacharyya, D. *Composites, Part A* **2004**, *35*, 1363−1374.
(14) Pothan, L. A.; Neelakantan, N. R; Thomas, S. *J. Reinf. Plast. Compos.* **1997**, *16* (8), 744−765.
(15) Zadorecki, P.; Flodin, P. *J. Appl. Polym. Sci.* **1985**, *30*, 3971.
(16) Zadorecki, P.; Rouhult, T. *J. Polym. Sci, Part A: Polym. Chem.* **1986**, *24*, 735.
(17) Shirley, D. A. *Phys. Rev. B* **1972**, *5*, 4709−4714.
(18) Jacobasch, H. J.; Simon, F.; Werner, C.; Bellmann, C. *Tech. Mess.* **1996**, *63*, 439−446.
(19) Spange, S.; Keutel, D.; Simon, F. *J. Chim. Phys. Phys.-Chim. Biol.* **1992**, *89*, 1615−1622.
(20) Spange, S.; Vilsmeier, E.; Fischer, K.; Reuter, A.; Prause, S.; Zimmermann, Y.; Schmidt, C. *Macromol. Rapid Commun.* **2000**, *21*, 643−659.
(21) Spange, S.; Vilsmeier, E.; Adolph, S.; Fährmann, A. *J. Phys. Org. Chem.* **1999**, *12*, 547−556.
(22) Pothan, L. A.; Zimmermann, Y.; Thomas, S.; Spange, S. *J. Polym. Sci., Part B: Polym. Phys.* **2000**, *38*, 2534−2553.
(23) Beamson, G.; Briggs, D. *High-Resolution of Organic Polymers, The Sienta ESCA 300 Database*; J. Wiley & Sons: Chichester, U.K., 1992; Appendix 1.
(24) Stern, O. *Z. Elektrochem.* **1924**, *30*, 508−516.

BM050462A